

Study of the Chemical Diversity in *Spondias tuberosa* Leaves During the Phenological Evolution Stages: Metabolomic and Chemometric Approaches Associated with Antioxidant and Antiglycant Activities

Francisco Wendell M. do Nascimento,^a Tamyrís A. Gondim,^a Paulo R. V. Ribeiro,^b Maria Auxiliadora C. de Lima,^c Viseldo R. de Oliveira,^c João Francisco Câmara Neto,^d Maria Elenir N. P. Ribeiro,^d Anna Beatriz S. Ferrari,^e Maria Luíza Zeraik,^{b,e} Jhonyson A. C. Guedes^{b,a} and Guilherme J. Zocolo^{b*,b,f}

^aLaboratório de Cromatografia, Departamento de Química Analítica e Físico-Química, Campus do Pici, Universidade Federal do Ceará (UFC), 60440-900 Fortaleza-CE, Brazil

^bEmbrapa Agroindústria Tropical, Rua Dra. Sara Mesquita, 2270, Pici, 60020-181 Fortaleza-CE, Brazil

^cEmbrapa Semiárido, Rodovia BR-428, Km 152, Zona Rural, 56302-970 Petrolina-PE, Brazil

^dLaboratório de Polímeros e Inovação de Materiais, Departamento de Química Orgânica e Inorgânica, Campus do Pici, Universidade Federal do Ceará (UFC), 60440-900 Fortaleza-CE, Brazil

^eLaboratório de Fitoquímica e Biomoléculas (LabFitoBio), Centro de Ciências Exatas (CCE), Universidade Estadual de Londrina (UEL), 86057-970 Londrina-PR, Brazil

^fEmbrapa Soja, 86001-970 Londrina-PR, Brazil

Spondias tuberosa (umbu) has been studied from the perspective of natural product and pharmacology, revealing relevant biological activities. Therefore, from the point of view of chemical and biological studies, deepening knowledge about this species is of great importance. Additionally, the evaluation related to the metabolic variations of the same species during different phenological evolution stages is also an interesting aspect of the research. Thereby, ultra-performance liquid chromatography coupled to mass spectrometry (UPLC-QToF-MS^E) was used to trace the chemical profile from umbu leaves at different phenological stages, allowing the detection of 40 metabolites, which 16 were annotated, such as phenolics and anacardic acids. Furthermore, the use of chemoinformatics tools allowed obtaining information on phenological development in the three leaves phases: post-flowering (young leaves), full production and senescence. The antiglycation activity assay revealed a potential inhibition of the formation of advanced glycation end-products (AGEs) in the leaves at different phenological stages. The antioxidant activity was satisfactory and in agreement with previously reported results, evidencing the potential for using umbu leaves, currently completely discarded, as an alternative source of antioxidants, which may provide increased added value to the cultivation of umbu, stimulating family farming and the recovery of tree density in degraded areas.

Keywords: umbu, liquid chromatography, multivariate analysis, mass spectrometry, metabolic variation

Introduction

Spondias tuberosa Arr., popularly known as umbuzeiro, is an endemic species of the Caatinga biome in Brazil, belonging to the Anacardiaceae family, which is distributed

mainly in the Northeast region of Brazil. Cultivated in low-income areas of Brazil, the fruits of *S. tuberosa* have high sociocultural importance in the semiarid region of Brazil, playing a crucial role as a source of subsistence for several family groups in these locations.¹ Its fruits are marketed both *in natura* and in processed form, as pulps, juices and other food products. In addition to their commercial use, they are widely recognized in folk medicine for the

*e-mail: guilherme.zocolo@embrapa.br

Editor handled this article: Andrea R. Chaves (Associate)



treatment of several conditions, including infections, venereal diseases, digestive disorders, diabetes, in addition to having antiemetic and tonic properties.^{2,3}

The literature reports that plants have the physiological capacity to synthesize a significantly greater amount of metabolites compared to most other living beings. These compounds are effective in reducing cellular and physiological oxidative stress caused by various disorders. Additionally, these metabolites have the potential to act in the treatment and prevention of various diseases, standing out for their antioxidant compounds.⁴⁻⁶ The ability of antioxidants to inhibit reactive oxygen species and free radicals is crucial for the therapeutic approach of diseases associated with oxidative stress, such as cancer, cardiovascular, neurodegenerative and inflammatory diseases, immune system dysfunctions, diabetes in addition to contributing to the aging process.⁶⁻⁸

The chemical composition of *Spondias tuberosa*, in the pulp, peel, seeds and leaves, presents a remarkable antioxidant activity and free radical scavenging capacity, attributed to the presence of phenolic compounds. In addition, other bioactive compounds such as flavonoids, anthocyanins and carotenoids are reported. Other compounds recognized for their therapeutic properties, such as gallic acid, chlorogenic acid, protocatechuic acid, *p*-coumaric acid, vanillic acid and ferulic acid, have also been identified in *S. tuberosa*.^{3,9-12} It is known that the chemical composition of plants, as well as their different parts (leaves, branches, fruits, seeds and roots), is quite variable, being influenced by biotic and abiotic factors. In addition, the different stages of development of the plant organism can also be responsible for causing changes in the biosynthetic processes.

Therefore, in this study, we performed a metabolomic workflow on umbuzeiro leaves in different phenological phases, aiming to establish the metabolic profile of these samples for the determination of bioactive chemical species. The metabolic profile of the samples was analyzed by ultra-performance liquid chromatography coupled to high-resolution mass spectrometry (UPLC-HRMS). Additionally, the samples were subjected to antiglycation and antioxidant activity assays using the 2,2-diphenyl-1-picrylhydrazyl (DPPH) radical scanning method. In order to facilitate data interpretation, chemometric tools were used to highlight similarities and/or differences related to phenological development in the three leaves phases. This approach will allow a detailed understanding of the metabolites present, enhancing the discovery of new drugs based on scientific evidence, in addition to contributing to the understanding of the antioxidant and antiglycation properties associated with *Spondias tuberosa*.

Experimental

Plant material and chemicals

The solvents and reagents used in the development of the work were purchased from LiChrosolv® of the Sigma-Aldrich Chemical Company (St. Louis, MO, USA). In addition, high purity Milli-Q water (Billerica, MA, USA) was used for all methods.

Spondias tuberosa leaves were collected at the Germplasm Active Bank (BAG) of Umbu in Petrolina-PE, geographic coordinates 09°03'42.6"S and 40°18'49.3"W. Leaves samples were collected from 30 plant accessions of the species. Collections were carried out on different dates relating to the phenological stages of the plant. The collection of young leaves was carried out on November 20, 21 and 26, 2018 and December 4. The collection for leaves in full production was carried out on March 19, 21 and 25, 2019 and April 9, 2019. The collection for leaves in senescence was carried out on June 6, 2019.

Metabolic quenching of the samples was performed using liquid N₂, to interrupt enzymatic activity and maintain the properties at the time of collection. Then, the leaves were freeze-dried, ground in a knife mill and sieved through an 80 mesh sieve to standardize particle size. Subsequently, the samples were identified and stored.

Extract preparation for UPLC analysis

The extracts were obtained by liquid-liquid partition, with 50 mg of each sample being weighed into centrifuge tubes. Then, 4 mL of hexane (purity of 95%) were added with the aim of degreasing the sample, by extracting non-polar components present in the plant tissue that could compromise the quality of the chemical analysis. Then, homogenization was carried out for 1 min in a vortex mixer and after this time, the samples were placed in an ultrasonic bath for 20 min. Subsequently, 4 mL of an ethanol/water solution (7:3) were added, subjecting the samples to vortexing again for 1 min followed by 20 min in an ultrasonic bath. After the extraction procedure, the samples were centrifuged for 10 min at 3000 rpm for effective separation of the extract phases. Finally, 1 mL of the hydroethanolic extract was filtered through a 0.22 µm PTFE (polytetrafluoroethylene) filter, and the filtrate was collected in vials. In addition, quality control (QC) samples, which are the mixture of equal volumes (10 µL) of all samples involved in the analysis, were prepared.¹³⁻¹⁵

Preparation of extract to evaluate biological activities

The preparation of extracts for the evaluation of biological activities is similar to the preparation for UPLC analysis. Therefore, 1 g of each sample was weighed. After weighing, 8 mL of an ethanol/water solution (7:3) was added. The mixture was vortexed for 1 min, followed by ultrasonic bath for 20 min. The next step consisted of adding 4 mL of hexane, vortex for 1 min, and ultrasonic bathing for 20 min. After the extraction process, the ethanol/water fraction (7:3) was collected and filtered through a 0.22 μm PTFE filter. Subsequently, the extracts were subjected to vacuum drying with heating at 45 °C in an Eppendorf Concentrator Plus (Hamburg, Germany) in desiccator mode. After drying, the samples were stored in an ultrafreezer at -80 °C.

Analysis conditions applied to the ultra-performance liquid chromatography-electrospray ionization mode-coupled to quadrupole and time-of-flight mass analyzers (UPLC-ESI-QToF-MS^E) system

The analyzes were performed on an Acquity UPLC system coupled to a Quadrupole/time-of-flight (QToF) mass spectrometer (UPLC-QToF, Waters Corporation, Milford, MA, USA). Chromatographic separations were carried out by means of Acquity UPLC BEH column (150 mm \times 2.1 mm, 1.7 μm , Waters Corporation, Milford, MA, USA) with a fixed temperature of 40 °C. The binary gradient elution system consisted of water with 0.1% formic acid (A) and acetonitrile with 0.1% formic acid (B), with gradient ranging 0-22 min (2-95%) from B; 22.50-26.00 min (98%) of B; 26.50-29.50 min (2%) of B, flow rate of 0.3 mL min⁻¹ and sample injection volume of 5 μL .

Data acquisition in the QToF system was performed using electrospray ionization in negative mode (ESI⁻), in the range of m/z 110-1100 in MS and 110-1100 in MS/MS, source temperature at 120 °C, desolvation temperature 350 °C and desolvation gas flow of 500 L h⁻¹. The capillary voltage was 2.6 kV. Leucine enkephalin was used as lock mass. The MS^E (mass spectrometry with energy variation) centroid acquisition mode was used, with a voltage ramp from 20 to 40 V. The instrument was controlled by MassLynx v.4.1 software (Waters Corporation, Milford, MA, USA).¹⁶

Compound annotation

Data processing from UPLC-QToF-MS^E analyzes was carried out using MassLynx software version 4.1.¹⁶ In the annotation of metabolites, the chromatographic peaks and mass spectra were considered with a tolerance

of ± 0.05 min for retention time and ± 0.05 Da for mass, respectively. The metabolic profile of the species under study was established through the correlation of MS and MS/MS spectra, by dereplication of the compounds, which were previously identified according to literature data based on chemotaxonomy.

Multivariate analysis

Aiming to discriminate the chemical profiles obtained by UPLC-QToF-MS^E analysis of the species at different phenological stages, the data were processed by the MarkerLynx software. Subsequently, multivariate analysis was performed, where principal component analysis (PCA) and orthogonal partial least squares-discriminant analysis (OPLS-DA) were used. Multivariate analysis was performed under the following conditions: retention time window of 0.90 to 26.00 min, mass range of 110 to 1100 Da, and mass tolerance of 0.02 Da. Furthermore, the retention time (t_R) and mass-to-charge ratio (m/z) parameters were used to identify each signal in the multivariate analysis. An identification was assigned to each of the t_R - m/z pairs based on the elution order. The ion intensities of each detected peak were normalized to the sum of the peak intensities within that sample using MarkerLynx software.¹⁷

The dataset was mean centered and the Pareto scaling method was used to generate the PCA. The data comprising peak number (t_R - m/z pair), sample name and ion intensity were analyzed by PCA and OPLS-DA using the MarkerLynx software.¹⁷

Antiglycant activity assay

Antiglycating activity was determined using the bovine serum albumin (BSA)/methylglyoxal (MGO) assay according to the method described by Lunceford and Gugliucci,¹⁸ with some modifications. A solution of BSA (1 mg mL⁻¹) was prepared in sodium phosphate buffer (10 mmol L⁻¹), pH 7.4, containing sodium chloride (150 mmol L⁻¹). An MGO solution (5 mmol L⁻¹) and the extracts (300 $\mu\text{g mL}^{-1}$) were added to the BSA solution and after that, the mixture was incubated at 37 °C for three days. The samples were incubated with the presence and absence (negative control) of aminoguanidine (10 mmol L⁻¹). After incubation, the fluorescence of the samples was measured at the excitation maximum of 370 nm and emission maximum of 440 nm, and the percentage inhibition of AGEs (advanced glycation end products) formation was calculated by $[(\text{FL}_{\text{CN}} \text{FL}_{\text{bCN}}) - (\text{FL}_{\text{s}} \text{FL}_{\text{bs}})] / (\text{FL}_{\text{CN}} \text{FL}_{\text{bCN}}) \times 100$, where FL_{CN} and FL_{bCN} are the fluorescence intensities of the negative control mixture and its blank, respectively, and

FLs and FL_{bs} are the fluorescence intensities of the extract and its blank, respectively.¹⁹

For statistical analysis, the normality of the data sets was first analyzed using the Kolmogorov-Smirnov test. After this step, the analysis of variance (one-way ANOVA) was performed. The confidence interval adopted was 95%, that is, results with $p < 0.05$ were considered statistically significant. Statistical analyzes of the data were performed using GraphPad Prism software version 10.0.3 (GraphPad Software Inc., Boston, MA, USA).²⁰

Antioxidant activity assay

Antioxidant activity was evaluated by the DPPH (2,2-diphenyl-1-picrylhydrazyl) assay described by Brand-Williams *et al.*,²¹ with some modifications.²² The samples were initially solubilized in ethanol (70%), and several dilutions were subsequently prepared for the test (5,000-5 $\mu\text{g mL}^{-1}$). The efficient concentrations (EC₅₀) was calculated from equation 1.

$$\text{EC}_{50} (\%) = \left(\frac{[A_{\text{DPPH}} - (A_{\text{sample}} - A_{\text{concentration}})]}{A_{\text{DPPH}}} \right) \times 100 \quad (1)$$

where A_{DPPH} is the absorbance detected for the ethanolic solution of DPPH, A_{samples} are the absorbances obtained for the reaction mixtures, and $A_{\text{concentration}}$ are the absorbances obtained for each dilution (only with absolute ethanol) at the wavelength of 515 nm. The efficient concentrations (EC₅₀) were determined by linear regression of the new concentrations by their respective EC₅₀, at a wavelength of 515 nm. All tests were carried out in sextuplicates

for statistical evaluation and ascorbic acid was used as a reference substance for the experiment.

For statistical analysis, the presence of outlier values was initially investigated, followed by an analysis of the normality of the data sets using the Shapiro-Wilk test. After this stage, the following statistical tests were used: analysis of variance (one-way ANOVA), followed by Tukey's multiple comparisons post-test for normal mean values and Krushal-Wallis test followed by Dunn's test for data non-parametric. The confidence interval adopted was 95%, that is, results with $*p < 0.05$ were considered statistically significant, with other levels of significance also being considered ($**p < 0.01$; $***p < 0.001$ and $****p < 0.0001$). Statistical analyzes of the data were performed using GraphPad Prism software version 10.0.3 (GraphPad Software Inc., Boston, MA, USA).²⁰ All results were expressed as mean \pm standard deviation.²²

Results and Discussion

Analysis of the chemical profile of *Spondias tuberosa* leaves

The chemical profile of *S. tuberosa* leaves was established from the interpretation of the chromatograms in negative ionization mode (ESI⁻) (Figure 1), together with the MS and MS/MS mass spectra obtained from UPLC-ESI-QToF-MS^E. In order to facilitate data evaluation, the peaks were numbered according to the elution order. Table 1 shows 40 detected compounds, with 16 annotated metabolites in the samples, with their respective deprotonated ions $[M - H]^-$, fragment ions, error in parts *per* million (ppm) and their possible molecular formula.

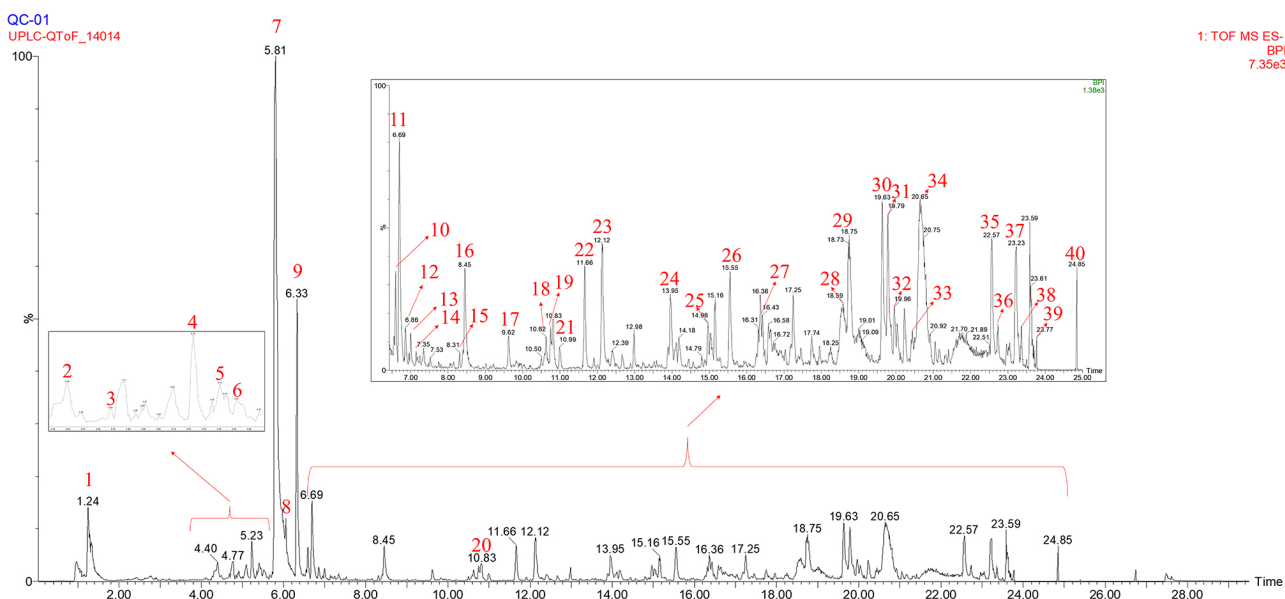


Figure 1. Representative chromatogram of *Spondias tuberosa* leaves obtained from UPLC-ESI-QToF-MS^E system in ESI⁻ mode.

Table 1. Annotated metabolites from *Spondias tuberosa* leaves extracts

Peak	t_R / min	[M - H] ⁻ observed	[M - H] ⁻ calculated	Product ions (MS/MS)	Molecular formula	Error / ppm	Annotated metabolites	Reference
1	1.24	189.0023	189.0035	171.9471; 127.0043	C ₆ H ₆ O ₇	-6.3	unidentified	
2	4.39	369.0468	369.0458	355.0773; 300.9883; 255.9643	C ₁₅ H ₁₄ O ₁₁	2.7	unidentified	
3	4.67	633.0708	633.0728	275.0167; 300.9948; 463.0451; 481.0250	C ₂₇ H ₂₂ O ₁₈	-3.2	corilagin	23
4	5.22	625.1427	625.1405	316.0241; 317.0344	C ₂₇ H ₃₀ O ₁₇	3.5	myricetin- <i>O</i> -rutinoside	24
5	5.40	953.0878	953.0896	935.1250; 633.0554; 463.0796; 169.0150	C ₄₁ H ₃₀ O ₂₇	-1.9	galloyl-hexahydroxydiphenoyl glucose	25
6	5.52	799.162	799.1628	609.1447; 189.0005	C ₂₆ H ₄₀ O ₂₈	-1.0	unidentified	
7	5.78	609.1484	609.1456	151.0026; 271.0276; 300.0245; 301.0305	C ₂₇ H ₃₀ O ₁₆	4.9	quercetin-3- <i>O</i> -rutinoside (rutin)	26
8	6.05	463.0853	463.0877	151.0024; 179.0019; 255.0322; 271.0221; 300.0256	C ₂₁ H ₂₀ O ₁₂	-5.2	quercetin-3- <i>O</i> -hexoside	26
9	6.33	593.1502	593.1506	255.0310; 284.0303; 285.0363	C ₂₇ H ₃₀ O ₁₅	-0.7	kaempferol 3- <i>O</i> -rutinoside	26
10	6.59	451.1655	451.1663	447.0905; 301.0267; 285.0391	C ₁₅ H ₃₂ O ₁₅	-1.8	unidentified	
11	6.69	615.1019	615.0986	301.0359; 463.0867	C ₂₈ H ₂₄ O ₁₆	5.4	quercetin galloyl hexoside	26
12	6.84	285.0422	285.0399	133.0407; 151.0080; 175.0382; 199.0362; 217.0973	C ₁₅ H ₁₀ O ₇	8.1	luteolin	24
13	6.98	293.0882	293.0873	273.1248; 189.0017; 149.0438	C ₁₁ H ₁₈ O ₉	3.1	unidentified	
14	7.14	745.2008	745.198	635.1664; 609.1448; 593.1516	C ₃₅ H ₃₈ O ₁₈	3.8	unidentified	
15	8.31	427.1867	427.1909	265.1380; 221.1516; 188.9999	C ₂₈ H ₂₈ O ₄	-9.8	unidentified	
16	8.44	301.0327	301.0348	273.0378; 229.0404; 178.9965; 151.0001; 121.0284	C ₁₅ H ₁₀ O ₇	-7.0	quercetin	24
17	9.60	285.0425	285.0399	151.0078; 229.0562; 257.0514	C ₁₅ H ₁₀ O ₆	9.1	kaempferol	24
18	10.61	329.2333	329.2328	285.0022; 265.1159; 241.0123; 203.1070	C ₁₈ H ₃₅ O ₅	1.5	unidentified	
19	10.74	287.2243	287.2222	269.2075; 217.0094; 197.1135	C ₁₆ H ₃₂ O ₄	7.3	unidentified	
20	10.82	287.2221	287.2222	269.2278; 255.2399; 189.0095; 127.0093	C ₁₆ H ₃₂ O ₄	-0.3	unidentified	
21	11.00	207.1385	207.1385	205.1189; 201.1330; 197.1153; 183.0070	C ₁₃ H ₂₀ O ₂	0.0	unidentified	
22	11.66	217.1233	235.1229	189.1280; 119.0459	C ₁₄ H ₁₈ O ₂	6.0	unidentified	
23	12.13	221.0597	221.0603	177.0686	C ₁₅ H ₁₀ O ₂	-2.7	9-anthracenecarboxylic acid	analytical standard
24	13.95	421.263	421.259	277.1931; 259.1728; 231.1743; 219.1394	C ₂₄ H ₃₈ O ₆	9.5	unidentified	
25	14.96	675.3482	675.3533	277.2115; 397.1243; 421.2523; 535.2705	C ₄₉ H ₅₂ O ₉	-7.6	unidentified	
26	15.56	593.2737	593.2751	277.2160; 241.0094; 152.9943	C ₃₄ H ₄₂ O ₉	-2.4	unidentified	
27	16.41	277.2161	277.2168	253.0880; 219.1403; 183.0102; 152.9970	C ₁₈ H ₃₀ O ₂	-2.5	unidentified	

Table 1. Annotated metabolites from *Spondias tuberosa* leaves extracts (cont.)

Peak	t_R / min	[M - H] ⁻ observed	[M - H] ⁻ calculated	Product ions (MS/MS)	Molecular formula	Error / ppm	Annotated metabolites	Reference
28	18.54	311.1688	311.1706	255.2302; 183.0088	C ₁₃ H ₂₈ O ₈	-5.8	unidentified	
29	18.74	571.2872	571.2848	255.2315; 241.0122; 183.0107; 152.9940	C ₁₃ H ₂₈ O ₈	-6.7	unidentified	
30	19.63	387.2526	387.2535	343.2630; 325.2425; 311.1680; 243.1733	C ₂₄ H ₃₆ O ₄	-2.3	unidentified	
31	19.78	387.2501	387.2535	325.2515; 233.1529; 219.1379; 183.0099	C ₂₄ H ₃₆ O ₄	-8.8	unidentified	
32	19.96	385.2372	385.2379	341.2468; 255.2275; 243.1719; 183.0058	C ₂₄ H ₃₆ O ₄	-7.5	unidentified	
33	20.26	385.2371	385.2379	255.2327; 233.1516; 183.0095; 152.9945	C ₂₄ H ₃₄ O ₄	-1.8	unidentified	
34	20.63	555.285	555.2805	225.0049	C ₂₈ H ₄₄ O ₁₁	8.1	unidentified	
35	22.55	369.2404	369.243	183.0098; 325.2491	C ₂₄ H ₃₄ O ₃	-7.0	anacardic acid (17:3)	27
36	22.73	343.2622	343.2637	183.0089	C ₂₃ H ₃₆ O ₂	-4.4	unidentified	
37	23.23	319.228	319.2273	275.2367	C ₂₀ H ₃₂ O ₃	2.2	anacardic acid (13:0)	27
38	23.35	345.2426	345.243	301.2552	C ₂₂ H ₃₄ O ₃	-1.2	anacardic acid (15:1)	27
39	23.77	371.2586	371.2586	327.2678	C ₂₄ H ₃₆ O ₃	0.0	anacardic acid (17:2)	27
40	24.85	373.2691	373.2743	329.2859	C ₂₄ H ₃₈ O ₃	-13.9	anacardic acid (17:1)	27

t_R : retention time.

In general, the metabolic profiles of the different phenological stages of *S. tuberosa* leaves presented a similar composition. Among the annotated metabolites, it was possible to observe several classes of compounds, such as polyphenols, ellagitannins, aglycone flavonoids, glycosylated flavonoids and anacardic acids. The description of the metabolite annotations is available in the Supplementary Information section.

Multivariate analysis

Principal component analysis (PCA)

PCA was initially used to reduce data complexity without losing important information. Score and loading graphs were used to investigate the relationship between the annotated compounds and the analyzed samples, to verify similarities and differences between the samples, resulting in the formation of possible clusters.³

As mentioned previously, in general, the samples present a similar chemical composition. However, with PCA it was possible to evaluate and infer the particularities of the sample groups, Figure 2. Thus, PC1 and PC2 allowed visualization of the behavior of the samples during the different phenological stages, with a cumulative explained variance of 39.47% ($R^2X[1] = 0.3118$ and $R^2X[2] = 0.0829$).

From the PCA score graph (Figure 2), it is possible to investigate the correlation of the samples with the phenological stages. In general, the observed behavior leads

us to infer that the data set is modeled based on the year of collection. Since we can verify the formation of a cluster, corresponding to the young leaves collected in spring 2018. This group is characterized by presenting a high correlation between the samples, given that the uniformity of the group is clear. On the other hand, there is a dispersion between the samples that make up the other three groups of samples (collection 2019), which results in a partial overlap of them. Thus, we can see that the group referring to the young leaves is the stage that differed the most from the others, being located exclusively in the negative of PC1 and PC2.

According to Gobbo-Neto and Lopes,²⁸ even though newer tissues have higher biosynthetic rates, an interesting phenomenon is observed: during periods of rapid tissue growth, there is a decrease in the production of certain specialized metabolites, notably phenolic derivatives. This fact suggests that when the plant is in the process of rapid growth, energy or resources can be diverted from some metabolic routes to support growth, therefore, the separation observed in the PCA score graph (Figure 2) may be related to the previously mentioned needs of young leaves.

However, when analyzing the other stages, there was a lower correlation between the samples and a greater correlation between the stages, making it possible to visualize a less pronounced transition between the stage of full production and senescence. According to studies by Aidar *et al.*,²⁹ on the phenology of umbuzeiro in the 2012-2013, 2013-2014, and 2014-2015 harvests, it was

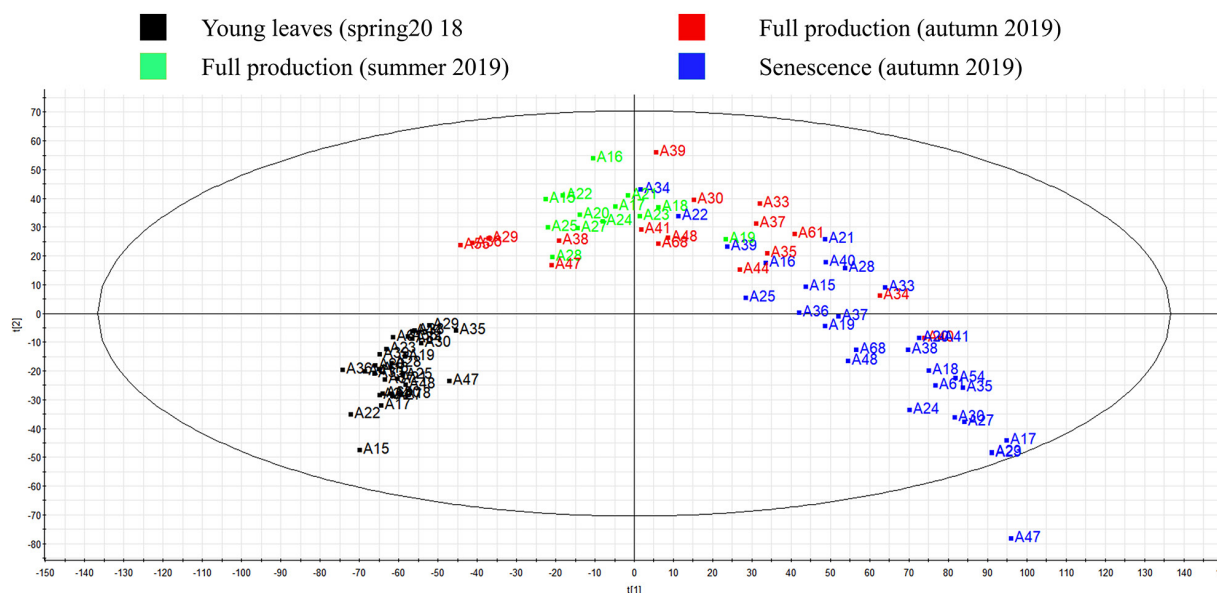


Figure 2. Principal component analysis (PCA), scores plot of leaves extracts from *Spondias tuberosa*.

possible to observe that the senescence process of the leaves began before the end of the period of fruit ripening, therefore, the correlation found between full production and senescence may be related to these processes occurring simultaneously in the plant.

The literature reports²⁹ that with the increase in the intensity of light incidence and the transition from the rainy to the dry period, the umbuzeiro enters a period of change from the growth phase to the vegetative rest phase. The progressive water deficit in the soil generally leads the plant to the senescence stage, a period in which several tissue photo-oxidation processes occur at an intensity in which the antioxidant photoprotection systems of the leaves are not sufficient to prevent the damage resulting from these processes. Furthermore, some studies³⁰ report that drought is one of the main factors that influence the quality and yield of plants, particularly affecting the accumulation of bioactive compounds in plants, leading to significant changes in the composition of phenolics present in the chemical composition of plants.

Although it is possible to identify sample groupings and correlations with phenological stages, a variety of distribution is observed within the same stage, with the possibility of being caused by the wide genetic variety of the specimens that make up the Germplasm Active Bank of (BAG). This assumption can be corroborated by the following example: some specimens produce fruits with great variability in mass, approximately 4 to 85 g, and with different flavors. In this context, the BAG is constituted of 80 accessions, representing all landscape units of the Northeastern Semiarid region, collected in the states of Pernambuco, Bahia, Minas Gerais, and Rio Grande do Norte.^{31,32}

The results obtained from PCA showed that the concentration of different compounds was directly affected by the collection period, and this difference may be related to the environmental conditions characteristic of each period, such as temperature, solar radiation, relative humidity, and rain, in addition to genetic factors, taking into account the different origins of the umbuzeiro accessions studied.

Orthogonal partial least squares-discriminant analysis (OPLS-DA)

Through PCA it was possible to clearly observe a group corresponding to the young leaves (collected in spring 2018) and the other three groups partially overlapping. However, to determine the responsible variables, chemical markers, for the separation and consequent differentiation of groups of samples, OPLS-DA associated with S-Plot scatter plots were used in the data set.

The evaluation of the OPLS-DA score graph between the samples in the phenological stage of young leaves, spring 2018, and senescence, autumn 2019, of *S. tuberosa* (Figure 3a), showed an explicit separation of the two sample groups. The model presented $R^2X = 0.98$ (explained variation) and $Q^2 = 0.97$ (predicted variation), suggesting that the model explains 98% of the variations in X, with a predictive capacity of 97%, indicating that the model is well established and has an excellent prediction. The identification of possible chemical markers was designed using S-Plot and variable importance in projection (VIP), which were obtained from OPLS-DA. In this work, the chemical markers with statistical significance presented $VIP > 7$ and $p < 0.05$ (Table 2).

Table 2. Chemical markers of the different phenological stages of *Spondias tuberosa* leaves

Peak	t_R / min	m/z	Metabolite	VIP			
				Young leaves (spring 2018) compared to senescence (autumn 2019)		Young leaves (spring 2018) compared to full production (summer and autumn 2019)	
				Young leaves (spring 2018)	Senescence (autumn 2019)	Young leaves (spring 2018)	Full production (summer and autumn 2019)
4	5.22	625.1427	myricetin- <i>O</i> -rutinoside	8.43		10.30	
5	5.40	953.0878	galloyl-hexahydroxydiphenoyl (HHDP) glucose			7.76	
7	5.78	609.1484	quercetin-3- <i>O</i> -rutinoside (rutin)		12.22		8.31
9	6.33	593.1502	kaempferol-3- <i>O</i> -rutinoside	14.75		9.34	
16	8.44	301.0327	quercetin	7.00		8.31	
22	11.66	217.1233	unidentified		9.11		
26	15.56	593.2737	unidentified	8.65		8.26	
27	16.41	277.2261	unidentified			7.30	
30	19.63	387.2526	unidentified		8.01		10.08
32	19.96	385.2372	unidentified		7.20		
34	20.63	555.2850	unidentified				9.85
35	22.55	369.2404	anacardic acid (17:3)	7.00			

t_R : retention time; VIP: variable importance in projection.

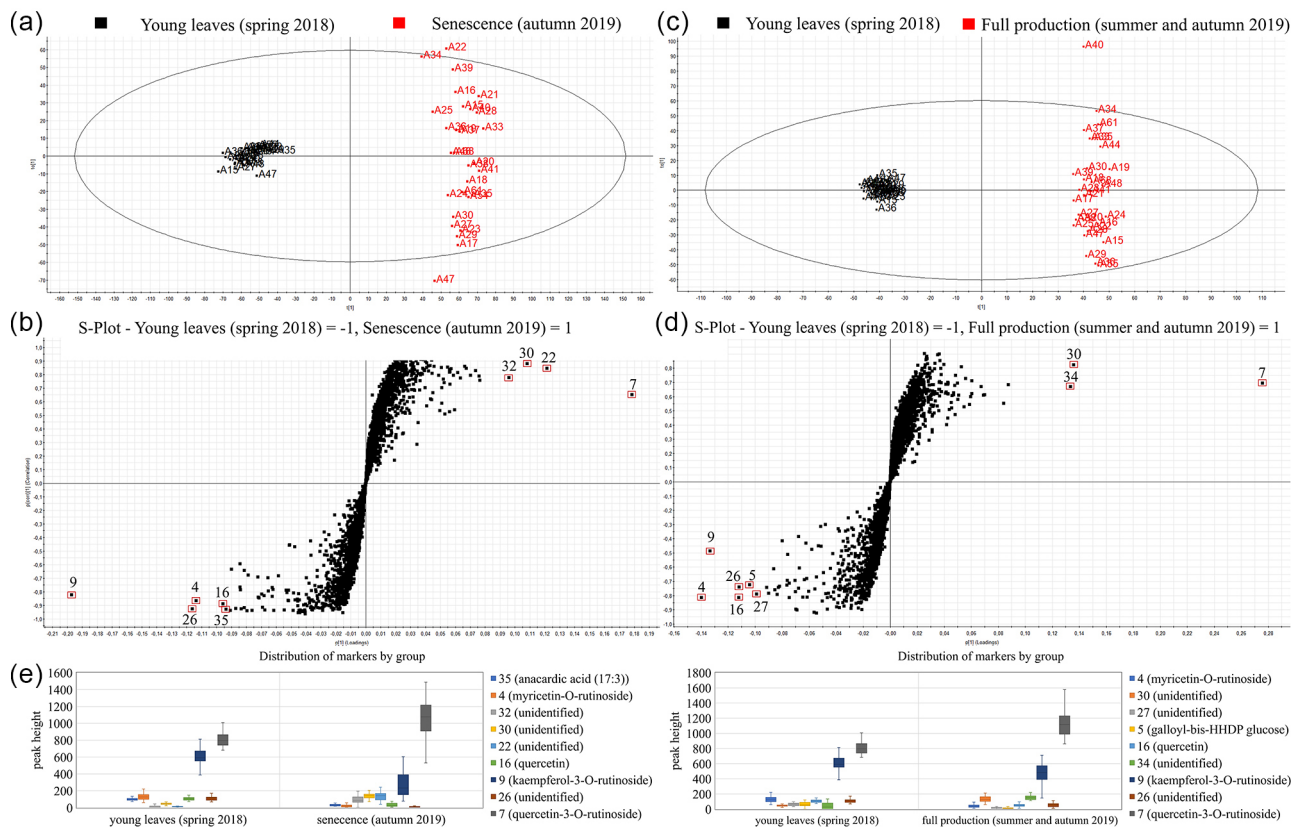


Figure 3. Graphs of multivariate analysis of *Spondias tuberosa* leaves extracts: (a) OPLS-DA young leaves compared with senescence; (b) S-Plot young leaves compared with senescence; (c) OPLS-DA young leaves compared with full production; (d) S-Plot young leaves compared with full production; and (e) average variation of chemical markers of the hydroethanolic extract from *Spondias tuberosa* leaves.

According to the S-Plot (Figure 3b), the ions in the lower left corner, represented by **4**, **9**, **16**, **26**, and **35** (Table 2), correspond to the metabolites with the greatest contribution to the characterization of the samples in the phenological stage young leaves spring 2018. On the other hand, in the upper right corner of the S-Plot graph (Figure 3b), compounds that contributed most to the characterization of samples in the senescence phenological stage of autumn 2019, were identified as **7**, **22**, **30**, and **32**. Therefore, the metabolites represented by **4**, **7**, **9**, **16**, **22**, **26**, **30**, **32**, and **35** are the potential chemical markers responsible for characterizing and discriminating the two groups of samples and consequently differentiating the samples in the phenological stage young leaves spring 2018 from the samples in the senescence phenological stage autumn 2019. The metabolites mentioned were annotated as myricetin-*O*-rutinoside (**4**), rutin (**7**), kaempferol 3-*O*-rutinoside (**9**), quercetin (**16**), unidentified (t_R 11.66 and m/z 217.1233) (**22**), unidentified (t_R 15.56 and m/z 593.2737) (**26**), unidentified (t_R 19.63 and m/z 387.2526) (**30**), unidentified (t_R 19.96 and m/z 385.2372) (**32**) and anacardic acid (17:3) (**35**).

In Figure 3c there is the OPLS-DA between the samples in the young leaves phenological stage (spring 2018) and the group containing the samples in the full production phenological stage (summer 2019 and autumn 2019). From OPLS-DA it was possible to verify a clear separation of the two sample groups, $R^2X = 0.99$ and $Q^2 = 0.96$. Therefore, the model explains 99% of the variations in X, with a predictive capacity of 96%, indicating that the model is well established and has excellent predictions.

The determination of chemical markers was carried out using the S-Plot (Figure 3d), the metabolites in the lower left corner, described by **4**, **5**, **9**, **16**, **26**, and **27** (Table 1) presented the greatest contribution for the characterization of samples at the phenological stage of young leaves (spring 2018). On the other hand, in the upper right corner of the S-Plot graph (Figure 3d), the compounds that most contributed to the characterization of the group containing the samples in the full production phenological stages (summer 2019 and autumn 2019) were metabolites **7**, **30** and **34**. Therefore, the compounds: myricetin-*O*-rutinoside (**4**), galloyl-hexahydroxydiphenoyl (HHDP) glucose (**5**), rutin (**7**), kaempferol 3-*O*-rutinoside (**9**), quercetin (**16**), unidentified (t_R 15.56 and m/z 593.2737) (**26**), unidentified (t_R 16.41 and m/z 277.2261) (**27**), unidentified (t_R 19.63 and m/z 387.2526) (**30**) and unidentified (t_R 20.63 and m/z 555.2850) (**34**) are the potential chemical markers responsible for characterizing and discriminating the two groups of samples and consequently differentiate the samples in the young leaves phenological stage (spring 2018) and the group containing the samples in the full

production phenological stage (summer 2019 and autumn 2019).

Table 2 shows the compounds annotated as discriminant based on the OPLS-DA and S-Plot analysis of young leaves compared with senescence and young leaves compared with full production, and their respective VIP values.

The evaluation of the chemical markers corresponding to the different phenological stages allowed us to verify that the phenolic compounds were the main variables responsible for the separation of the groups under study. Although they were classified as discriminant, phenolic compounds were present in all phenological stages, but at different concentration levels. A study conducted by Liu *et al.*,³³ demonstrated that there is variation in flavonoids, anthocyanins, and procyanidins during the development of *Zingiber mioga* flowers, explaining that the production of these constituents may be restricted to some specific stage of development of the plant. This fact suggests a complex interaction between phenological development and the biosynthesis of phenolic compounds, underlining the adaptive sophistication of these plants to variable environmental conditions and possibly specific ecological challenges.

Evaluation of the distribution of chemical markers in *S. tuberosa* leaves

The analysis of phenotypic variation in *S. tuberosa*, as illustrated in Figure 3e, reveals significant differences in the chemical composition of leaves at different phenological stages, evidencing the complex interaction between plant metabolism and seasonal environmental conditions. During the spring of 2018, a high concentration of flavonoids, such as myricetin-*O*-rutinoside, kaempferol 3-*O*-rutinoside, and quercetin, was observed. These compounds are known for their antioxidant properties, suggesting an adaptive response of the plant to the conditions of vigorous growth in spring, which requires protection against free radicals produced during intense metabolic processes. In contrast, in the autumn of 2019, marked by senescence, a reduction in these compounds was observed, possibly due to the natural degradation associated with leaves aging and preparation for winter dormancy. This suggests a decrease in metabolic activity and the need for antioxidant defenses as the plant prepares for adverse conditions.

Additionally, during the full production periods in the summer and autumn of 2019, elevated concentrations of rutin and other unidentified compounds were detected, indicative of a distinct metabolic profile that may be related to plant maturation and reproduction. These compounds may play crucial roles in protecting against heat stress and

attracting pollinators, which are essential for reproduction at the peak of the growing season.

Antiglycant activity assay

The hydroethanolic extracts of *Spondias tuberosa* leaves were tested for their antiglycation capacity. Initially, a screening was performed, where the extracts were tested at a concentration of 300 $\mu\text{g mL}^{-1}$ and the antiglycation activity was determined using fluorimetry, as described in the literature,¹⁹ due to the fluorescence exhibited by AGEs.

The extracts showed a highly diversified antiglycation capacity, ranging from 3.6-97.2% (Figure 4). It was possible to observe that this variation occurred both between the phenological stages and within the same stage. Among the samples tested, 71.76% were classified as active, demonstrating glycation inhibition greater than 50%, while 37.64% of the samples showed glycation inhibition greater than that of aminoguanidine (74.7%), used as a positive control due to its proven antiglycation activity. Regarding the young leaves stage, 73.33% were classified as active,

where 36.67% of the samples were superior to the positive control (Figure 4a). At the full production stage, 75% were classified as active and 46.42% were superior to the positive control (Figure 4b) finally at the senescence stage, 70.37% were classified as active and 44.44% were superior to the positive control (Figure 4c).

Specimens A19, A21, A34, A36, A39, and A47 showed high antiglycation activity in all phenological stages, higher than 74.7% of aminoguanidine, used as a positive control. Specimens A15, A16, A18, A22, A24, A28, A29, A38, A48, and A68 showed intermediate values of antiglycation activity, i.e., higher than 50%, up to high values, higher than 74.7% in all phenological stages. Specimens A17, A20, A23, A25, A27, A30, A35, A33, A37, A44 and A61 presented low values of antiglycation activity, that is, less than 50% up to values greater than 74.7%, where specimens A23, A27, A44, A61 presented only values below 50% of antiglycation activity.

The results of the mean antiglycation activity for the different phenological stages indicated the values of 62.74% for young leaves, 64.85% for full production, and 64.97% for

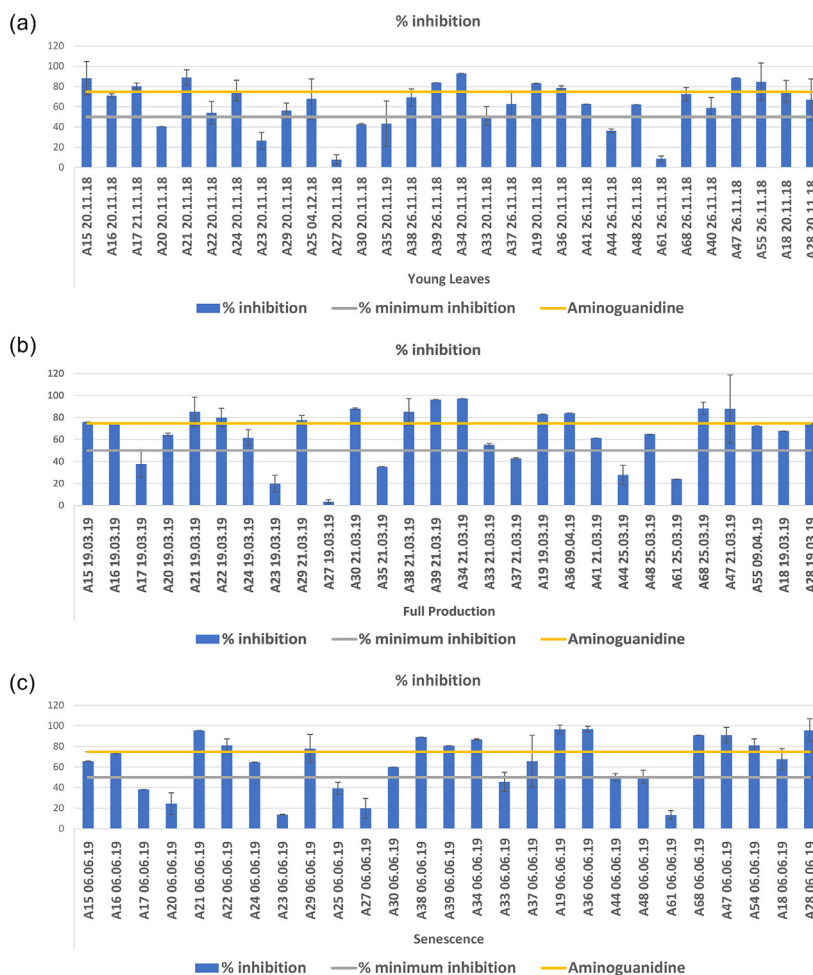


Figure 4. AGE inhibition percentages (a) young leaves; (b) full production and (c) senescence.

for the senescence stage. An ANOVA was performed to assess whether there was a significant difference between the means. Through the Kolmogorov-Smirnov normality test, the results showed a normal distribution, and thus, it was possible to perform the ANOVA. The data from the ANOVA are available in the Supplementary Information section, Table S1.

Therefore, through ANOVA it was possible to affirm that there is no significant difference between the means of the analyzed groups, that is, the leaves of *S. tuberosa* presented statistically the same antiglycation activity in all phenological stages studied in this work. Although the chemical composition of the umbu tree (*S. tuberosa*) is little known, it is known that several of the pharmacological properties of the genus *Spondias* are attributed to phenolic compounds, such as tannins and flavonoids, present mainly in the leaves.³ The use of *Spondias tuberosa* leaves in folk medicine for the treatment of various diseases, such as diabetes,³⁴ was in agreement with the results obtained since the formation of AGEs is one of the main mechanisms responsible for the cellular and tissue damage observed in this disease.³⁵

According to Galeno *et al.*,³⁶ compounds such as gallic acid, myricetin-3-rhamnoside, quercetin-3-*O*-galactoside, quercetin-3-*O*-xyloside, quercetin-3-*O*-rhamnoside, and kaempferol-3-*O*-rhamnoside, have a high antioxidant potential and have been associated with hypoglycemic therapeutic effects, enzyme inhibition (α -amylase, α -glucose and xanthine oxidase), as well as potential to reduce the risks of heart disease and type 2 diabetes mellitus. And as pointed out by Wu and Yen,³⁷ in addition to having antioxidant potential, flavonoids inhibit glyoxidation and, consequently, the formation of AGEs. The presence of some of these compounds already reported in umbuzeiro leaves by Guedes *et al.*,³ may be related to the antiglycation activity presented by *S. tuberosa* leaves, not yet reported in the literature. Furthermore, the literature³⁷ reports that phenolic compounds in the following increasing order kaempferol < quercetin < rutin < luteolin, have a high capacity to inhibit the formation of AGEs, where luteolin and kaempferol gained prominence due to their ability to break cross-links between AGEs and proteins.

As previously mentioned, the antiglycation activity of umbu leaves may be related to the phenolic compounds found in the plant. Additionally, the average variation of chemical markers distributed in the leaves of *S. tuberosa* at different phenological stages was seen in the previous section, and among the chemical markers, there are flavonoids such as myricetin-*O*-rhamnosylglucose, quercetin-3-*O*-rutinoside (rutin), kaempferol 3-*O*-rutinoside and quercetin (Figure 5).

The variation found in antiglycation activity may be directly related to the variation in the concentration of these flavonoids and their different ways of reducing the formation of AGEs, which can occur through two main pathways: influencing through antioxidant mechanisms and/or intervening in one or more stages of the biochemical pathways involved in the glycation reaction in the initial stages, where Amadori products are formed, intermediate, with the formation of reactive carbonyl species and final with the formation of AGEs and cross-linking.³⁷

According to Chinchansure *et al.*,³⁸ in the initial stage, rutin is capable of inhibiting the formation of the Schiff base, and in the second stage, quercetin is capable of inhibiting the formation of Amadori products, while in the post-Amadori stage, flavonoids such as luteolin and myricetin are capable of capturing the reactive carbonyl species that are involved in the cross-linking of proteins and the formation of AGEs. The hydroethanolic extracts of *S. tuberosa* leaves showed antiglycation activity, proving capable of reducing the interaction of methylglyoxal (MG) with bovine serum albumin (BSA), making them promising for use as natural sources of components in cosmetic or pharmaceutical formulations for the treatment of degenerative diseases and in combating premature aging since there is strong evidence that the glycation process of skin proteins, such as collagen, is directly involved in the aging process.³⁹

Antioxidant activity assay

The samples subjected to evaluation of antioxidant potential were selected based on the results obtained from antiglycant activity and PCA, Figure 2. The formation of three groups of specimens was observed, where in the first group, a high antiglycant activity was exhibited, in the second group an intermediate antiglycant activity was obtained and in the third group, the antiglycant activity exhibited was considered low. To correlate antiglycating activity with antioxidant activity, representative specimens were selected from each group, where specimens A34 (first group), A16 (second group), and A27 (third group) were chosen.

The samples chosen by PCA had the objective of measuring the contribution to the antioxidant activity of the substances that appeared at the ends of the loadings graph. Some of these substances were annotated as chemical markers such as myricetin-*O*-rhamnosylglucose, quercetin-3-*O*-rutinoside (rutin), kaempferol 3-*O*-rutinoside and unidentified (t_R 11.66 and m/z 217.1233). The results for the evaluated samples and the reference substance are shown in Table 3.

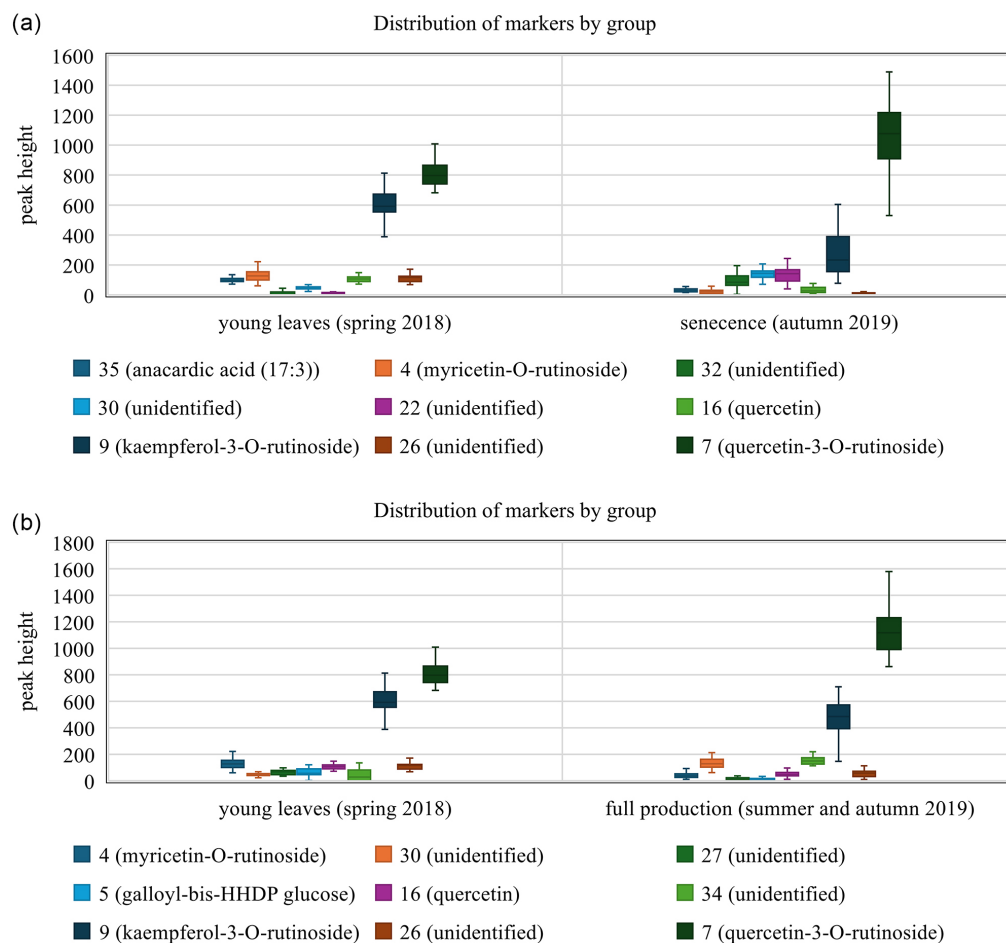


Figure 5. Distribution of chemical markers of umbu leaves, comparison between group of samples: (a) young leaves (spring 2018) with senescence (autumn 2019); (b) young leaves (spring 2018) with full production (summer and autumn 2019).

In the antioxidant activity test using the DPPH method, DPPH is used as a free radical to evaluate the antioxidant capacity of the extracts, and the degree of discoloration is attributed to the hydrogen atom donation capacity of the substances contained in these extracts.⁴⁰ The EC_{50} was used to categorize the antioxidant activities of the extracts and compare them with the standard used. Samples with $EC_{50} < 50 \mu\text{g mL}^{-1}$ are very strong antioxidants, $50\text{--}100 \mu\text{g mL}^{-1}$ are strong antioxidants, $101\text{--}150 \mu\text{g mL}^{-1}$ are moderate antioxidants and $> 150 \mu\text{g mL}^{-1}$ are considered weak antioxidants.⁴¹

As shown in Table 3, it was possible to observe that ethanolic extracts of *Spondias tuberosa* (A16 20/11/2018; A22 20/11/18; A27 20/11/18; A27 19/13/19; A27 06/06/19; A34 20/11/18; A34 21/03/19 and A55 09/04/19) exhibited $EC_{50} < 50 \mu\text{g mL}^{-1}$, therefore, they were categorized according to the previously mentioned classification as very strong antioxidants. Furthermore, the extracts (A16 03/19/19; A16 06/06/2019; A22 11/20/2018; A33 06/06/19 and A34 06/06/19) presented EC_{50} values of $50\text{--}100 \mu\text{g mL}^{-1}$, being classified as strong antioxidants. On

Table 3. Assessment of radical scavenging antioxidant capacity (DPPH) from extracts of *Spondias tuberosa* leaves

Sample	$EC_{50}^d / \%$	AGEs ^e inhibition / %
Ascorbic acid	7.8024 ± 0.0885	–
A16 (20/11/18) ^a	34.6800 ± 1.1700	71 ± 1.67
A16 (19/03/19) ^b	54.8413 ± 2.4142	74.8 ± 0.20
A16 (06/06/19) ^c	60.6534 ± 1.4365	73.2 ± 0.32
A17 (06/06/19) ^c	118.9237 ± 0.8518	38.2 ± 0.00
A22 (20/11/18) ^a	51.9838 ± 0.8395	54.2 ± 11.17
A27 (20/11/18) ^a	37.7482 ± 2.1772	7.8 ± 4.72
A27 (19/03/19) ^b	37.0000 ± 1.1230	3.6 ± 1.80
A27 (06/06/19) ^c	40.186 ± 0.6067	19.8 ± 9.67
A33 (06/06/19) ^c	61.7502 ± 1.7162	45.5 ± 9.29
A34 (20/11/18) ^a	34.5698 ± 4.3669	92.9 ± 0.00
A34 (21/03/19) ^b	47.5476 ± 0.6677	97.2 ± 0.00
A34 (06/06/19) ^c	63.1121 ± 1.0152	86.9 ± 0.47
A55 (09/04/19) ^b	49.2467 ± 1.2001	72.3 ± 0.00

^aYoung leaves; ^bfull production; ^csenescence; ^dhalf maximal inhibitory concentration; ^eadvanced glycation end products.

the other hand, the extract (A17 06/06/19) was the only one that presented EC_{50} values $> 100 \mu\text{g mL}^{-1}$, being classified as a moderate antioxidant.

The comparative analysis between the results obtained in the antiglycation activity test and the antioxidant activity results allowed us to observe that some samples showed completely different behaviors to the two activities tested (Table 3).

Specimen A17 (06/06/19) showed that there was no contribution of the unidentified constituent (t_R 11.66 and m/z 217.1233) to the antioxidant activity, presenting the highest EC_{50} of the specimens analyzed. On the other hand, specimen A22 (11/20/18) showed a significant contribution of the myricetin-*O*-rutinoside constituent to the antioxidant activity. In the case of specimen A33 (06/06/19), a good contribution of the constituent quercetin-3-*O*-rutinoside (rutin) to the antiglycation activity was verified, classifying the sample as a strong antioxidant according to the classification of Fidrianny *et al.*⁴² Specimen A55 (09/04/19) showed a strong contribution of the constituent kaempferol

3-*O*-rutinoside to the antioxidant activity, presenting $EC_{50} < 50 \mu\text{g mL}^{-1}$, classifying the sample as a very strong antioxidant.

Specimen A27 presented antiglycation activity of less than 50% in all phenological stages, the minimum inhibitory percentage to be considered active. In contrast, the same specimen obtained high performance in the antioxidant activity assay, deviating from the pattern observed for the other specimens. Through the average variation of the constituents of each specimen, the chemical composition of specimen A27 was compared to the chemical composition of specimen A34, which obtained high performance in both activities studied in this work (Figure 6). Thus, through the evaluation of the average variation of the constituents of specimens A27 and A34, which was obtained from an OPLS-DA, it was possible to verify that the composition presented similarity, however, the average concentration of the chemical components was different, and this variation may be related to the difference in activity observed.

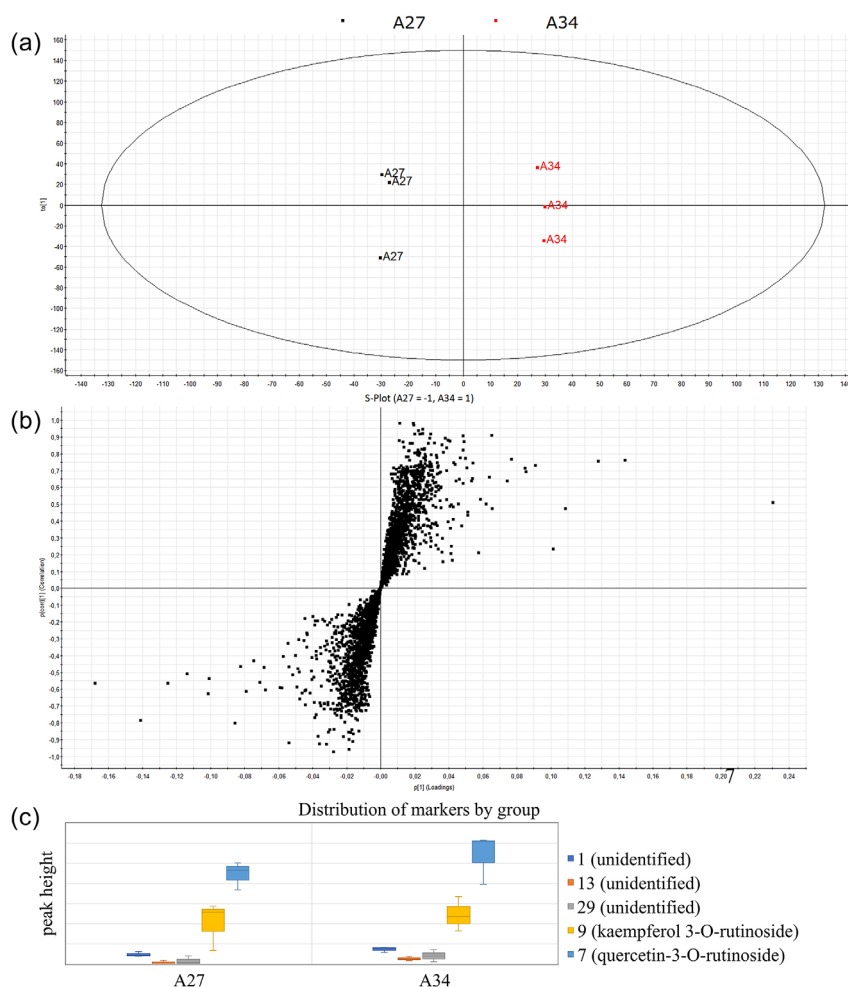


Figure 6. Multivariate analysis of *Spondias tuberosa* leaves samples: (a) OPLS-DA A27 compared with A34; (b) S-Plot A27 compared with A34; (c) average variation of chemical markers of A34 about A27.

The analysis of antioxidant (AO) and antiglycation (AG) activities presented in Table 3 reveals a remarkable pattern: while samples A27 and A34 exhibit high levels of AO activity, they differ significantly in AG activity: sample A27 shows low AG activity, unlike sample A34, which presents high levels of this activity. To find the compounds responsible for this difference in AG activity OPLS-DA was used, in Figures 6b and 6c. The application of this multivariate statistical tool allowed us to detect the marked presence of flavonoids, specifically quercetin-3-*O*-rutinoside (rutin) (**7**) and kaempferol-3-*O*-rutinoside (**9**), in sample A34, correlates with its superior performance in AG. Thus, the potential contribution of these flavonoids to the bioactive properties of the studied sample is highlighted. The ability of some flavonoids to inhibit the formation of AGEs and their specific antioxidant activities are directly related. However, some conflicts have been observed, such as the flavonoids apigenin, wogonin, and rhamnetin, which showed inhibitory activity against the formation of AGEs but exhibited low antioxidant activity.⁴³

In general, the capacity to sequester free radicals displayed by extracts from *S. tuberosa* leaves was satisfactory, therefore, its use in cosmetic formulations to prevent damage caused by reactive oxygen species may be a way to counterbalance the deleterious effect caused by oxidative stress.⁴⁴

Conclusions

Through UPLC-ESI-QTOF-MS^E, it was possible to trace the chemical profile of *S. tuberosa* leaves in the three phases: post-flowering phase (young leaves), full production, and senescence, in addition to allowing the annotation of 16 metabolites. Multivariate analysis (PCA, OPLS-DA, and S-Plot) proved to be essential to identify the differences and similarities of the metabolic profiles of *Spondias tuberosa* leaves in different phenological stages, enabling the identification of the chemical markers responsible for characterizing and discriminating the phenological stages of umbu leaves.

Regarding biological activity, it was observed that umbu leaves extracts presented antiglycant and antioxidant activity, highlighting their potential use as a source of natural antioxidants and antiglycants, making them candidates for use as an active ingredient in cosmetic formulations with anti-aging action.

Therefore, these observations are corroborated using advanced metabolomics techniques, which allow a detailed and quantitative analysis of metabolic profiles. The use of chemometrics in the studies, including principal component analyses and discriminant analyses, facilitates

the interpretation of these complex data, revealing not only significant biochemical variations between the different phenological stages, but also providing insights into the adaptive strategies of the plant in response to seasonal changes in the environment. This integrated approach is essential for a deeper understanding of cause-effect relationships in plant metabolism, offering valuable insights into plant biology and agronomic applications.

Supplementary Information

Supplementary information (description of annotated metabolites based on mass spectrometry and ANOVA table of antiglycation activity) is available free of charge at <http://jbcs.sbq.org.br> as PDF file.

Acknowledgments

The authors gratefully acknowledge the financial support from the CNPq, National Council for Scientific and Technological Development (303791/2016-0), INCT BioNat, National Institute of Science and Technology (grant No. 465637/2014-0). We would also like to thank Embrapa (SEG 03.14.01.012.00.00 and SEG 10.19.00.035.00.00). This study was financed in part by the Coordenação de Aperfeiçoamento de Pessoal de Nível Superior - Brasil (CAPES) - Finance Code 001 (PROEX 23038.000509/2020-82).

Author Contributions

Francisco Wendell M. do Nascimento for conceptualization, data curation, formal analysis, investigation, validation, visualization, writing original draft; Tamiris A. Gondim for conceptualization, investigation, validation, visualization, writing original draft, review and editing; Paulo R. V. Ribeiro for formal analysis, investigation, software, validation, visualization, writing original draft; Maria Auxiliadora C. de Lima for data curation, funding acquisition, resources, validation, visualization; Viseldo R. de Oliveira for data curation, funding acquisition, resources, validation, visualization; João Francisco Câmara Neto for conceptualization, formal analysis, investigation, validation, visualization, writing original draft; Maria Elenir N. P. Ribeiro for conceptualization, data curation, investigation, resources, validation, visualization, writing original draft; Anna Beatriz S. Ferrari for conceptualization, formal analysis, investigation, resources, validation, visualization, writing original draft; Maria Luiza Zeraik for conceptualization, formal analysis, investigation, resources, validation, visualization, writing original draft; Jhonyson A. C. Guedes for conceptualization, data curation, investigation, project administration, resources, software, validation, visualization, writing original draft, review and editing; Guilherme J. Zocolo for

conceptualization, data curation, funding acquisition, investigation, project administration, resources, validation, visualization, writing original draft, review and editing.

References

- Rodrigues, N. L.; Souza, A. L. C.; de Oliveira, C. C.; de Carvalho, M. G.; de Lima, B. R.; de Akutsu, R. C. C. A.; de Lana, V. S.; Raposo, A.; Saraiva, A.; Han, H.; de Carvalho, I. M. M.; *J. Food Compos. Anal.* **2024**, *130*, 106196. [Crossref]
- de Albuquerque, U. P.; de Medeiros, P. M.; de Almeida, A. L. S.; Monteiro, J. M.; Lins Neto, E. M. F.; de Melo, J. G.; dos Santos, J. P.; *J. Ethnopharmacol.* **2007**, *114*, 325. [Crossref]
- Guedes, J. A. C.; Santiago, Y. G.; Luz, L. R.; Silva, M. F. S.; Ramires, C. M. C.; de Lima, M. A. C.; de Oliveira, V. R.; do Ó Pessoa, C.; Canuto, K. M.; de Brito, E. S.; F. Lima, M.; Alves, R. E.; Zampieri, D.; do Nascimento, R. F.; Zocolo, G. J.; *Phytochem. Lett.* **2020**, *40*, 26. [Crossref]
- Alseekh, S.; Fernie, A. R.; *Plant J.* **2018**, *94*, 933. [Crossref]
- Wang, S.; Li, Y.; He, L.; Yang, J.; Fernie, A. R.; Luo, J.; *Curr. Opin. Plant Biol.* **2022**, *67*, 102201. [Crossref]
- Bras, B. S.; Pereira, I. N.; Zibordi, L. C.; Rosatto, P. A. P.; Santos, H. H.; Granero, F. O.; Figueiredo, C. C. M.; de Faria, M. L.; Ximenes, V. F.; de Moraes, R. O.; Santiago, P. S.; Nicolau-Junior, N.; Silva, L. P.; Silva, R. M. G.; *Food Bioprod. Process.* **2024**, *147*, 175. [Crossref]
- Feng, A.; Zhao, Z.; Liu, C.; Du, C.; Gao, P.; Liu, X.; Li, D.; *Int. J. Biol. Macromol.* **2024**, *266*, 131171. [Crossref]
- Jabbar, A.; Ilyas Y, M.; Wahyuni; Hamzah, H.; Windarsih, A.; Pratiwi, S. U. T.; Rohman, A.; *Case Stud. Chem. Environ. Eng.* **2024**, *10*, 100780. [Crossref]
- Dias, J. L.; Mazzutti, S.; de Souza, J. A. L.; Ferreira, S. R. S.; Soares, L. A. L.; Stragevitch, L.; Danielski, L.; *J. Supercrit. Fluids* **2019**, *145*, 10. [Crossref]
- Guedes, J. A. C.; Alves Filho, E. G.; Silva, M. F. S.; Rodrigues, T. H. S.; Ramires, C. M. C.; Lima, M. A. C.; Silva, G. S.; Pessoa, C. Ó.; Canuto, K. M.; Brito, E. S.; Alves, R. E.; Nascimento, R. F.; Zocolo, G. J.; *J. Braz. Chem. Soc.* **2020**, *31*, 331. [Crossref]
- Cordeiro, B. M. C. P.; Santos, N. D. L.; Ferreira, M. R. A.; de Araújo, L. C. C.; Carvalho Jr., A. R.; Santos, A. D. C.; de Oliveira, A. P.; da Silva, A. G.; Falcão, E. P. S.; Correia, M. T. S.; Almeida, J. R. G. S.; da Silva, L. C. N.; Soares, L. A. L.; Napoleão, T. H.; da Silva, M. V.; Paiva, P. M. G.; *BMC Complement. Altern. Med.* **2018**, *18*, 284. [Crossref]
- Barbosa, H. de M.; Amaral, D.; do Nascimento, J. N.; Machado, D. C.; de Sousa Araújo, T. A.; de Albuquerque, U. P.; Almeida, J. R. G. S.; Rolim, L. A.; Lopes, N. P.; Gomes, D. A.; Lira, E. C.; *J. Ethnopharmacol.* **2018**, *227*, 248. [Crossref]
- Gondim, T. A.; Guedes, J. A. C.; Alves Filho, E. G.; da Silva, G. S.; Nina, N. V. S.; do Nascimento Filho, F. J.; Atroch, A. L.; da Silva, G. F.; Lopes, G. S.; Zocolo, G. J.; *Anal. Methods* **2023**, *16*, 1158. [Crossref] [PubMed]
- Gondim, T. A.; Guedes, J. A. C.; Silva, M. F. S.; da Silva, A. C.; Dionísio, A. P.; Souza, F. V. D.; do Ó Pessoa, C.; Lopes, G. S.; Zocolo, G. J.; *Food Res. Int.* **2023**, *164*, 112439. [Crossref]
- Chagas-Paula, D. A.; Zhang, T.; da Costa, F. B.; Edrada-Ebel, R. A.; *Metabolites* **2015**, *5*, 404. [Crossref] [PubMed]
- MassLynx*, v.4.1; Waters Corporation, Milford, USA, 2009.
- MarkerLynx*, XS v.4.1; Waters Corporation, Milford, USA, 2009.
- Lunceford, N.; Gugliucci, A.; *Fitoterapia* **2005**, *76*, 419. [Crossref]
- Fraige, K.; Dametto, A. C.; Zeraik, M. L.; de Freitas, L.; Saraiva, A. C.; Medeiros, A. I.; Castro-Gamboa, I.; Cavalheiro, A. J.; Silva, D. H. S.; Lopes, N. P.; Bolzani, V. S.; *Phytochem. Anal.* **2018**, *29*, 196. [Crossref]
- GraphPad Prism*, v.10.0.3; GraphPad Software, Boston, USA, 2023.
- Brand-Williams, W.; Cuvelier, M. E.; Berset, C.; *LWT - Food Sci. Technol.* **1995**, *28*, 25. [Crossref]
- Câmara Neto, J. F.; Campelo, M. S.; de Cerqueira, G. S. L.; Miranda, J. A.; Guedes, J. A. C.; de Almeida, R. R.; Soares, S. A.; Gramosa, N. V.; Zocolo, G. J.; Vieira, Í. G. P.; Ricardo, N. M. P. S.; Ribeiro, M. E. N. P.; *J. Ethnopharmacol.* **2022**, *292*, 115191. [Crossref]
- Kumar, S.; Chandra, P.; Bajpai, V.; Singh, A.; Srivastava, M.; Mishra, D. K. K.; Kumar, B.; *Ind. Crops Prod.* **2015**, *69*, 143. [Crossref]
- Abu-Reidah, I. M.; Ali-shtayeh, M. S.; Jamous, R. M.; Arráez-Román, D.; Segura-carretero, A.; *Food Chem.* **2015**, *166*, 179. [Crossref] [PubMed]
- da Silva, J. A.; Donato, S. L. R.; Donato, P. E. R.; Souza, E. S.; Padilha Jr., M. C.; e Silva Jr., A. A.; *Rev. Bras. Eng. Agríc. Ambient.* **2016**, *20*, 236. [Crossref]
- Engels, C.; Gräter, D.; Esquivel, P.; Jiménez, V. M.; Gänzle, M. G.; Schieber, A.; *Food Res. Int.* **2012**, *46*, 557. [Crossref]
- Ersan, S.; Üstünda, Ö. G.; Carle, R.; Schweiggert, R. M.; *J. Agric. Food Chem.* **2016**, *64*, 5334. [Crossref]
- Gobbo-Neto, L.; Lopes, N. P.; *Quim. Nova* **2007**, *30*, 374. [Crossref]
- Aidar, S. T.; Chaves, A. R. M.; de Lima, M. A. C.; de Araújo, F. P.; *Fenologia, Produção e Características Químicas dos Frutos de Acessos de Umbuzeiro (Spondias tuberosa Arruda) em Petrolina, PE*; Embrapa Semiárido: Petrolina, 2021. [Link] accessed in November 2024
- Zanatta, A. C.; Vilegas, W.; Edrada-Ebel, R.; *Front. Chem.* **2021**, *9*, 710025. [Crossref]
- Santos, C. A. F.; Nascimento, C. E. D. S.; Campos, C. D. O.; *Rev. Bras. Frutic.* **1999**, *21*, 104. [Link] accessed in November 2024

32. da Silva Jr., J. F.; Souza, F. V. D.; Pádua, J. G.; *A Arca de Noé das Frutas Nativas Brasileiras*; Embrapa: Brasília, 2021. [Link] accessed in November 2024
33. Liu, H.; Cheng, Z.; Luo, M.; Xie, J.; *J. Food Compos. Anal.* **2023**, *123*, 105537. [Crossref]
34. Agra, M. F.; de Freitas, P. F.; Barbosa-Filho, J. M.; *Rev. Bras. Farmacogn.* **2007**, *17*, 114. [Crossref]
35. Jakuš, V.; Rietbrock, N.; *Physiol. Res.* **2004**, *53*, 131. [Crossref] [PubMed]
36. Galeno, D. M. L.; Carvalho, R. P.; de Araújo Boleti, A. P.; Lima, A. S.; de Almeida, P. D. O.; Pacheco, C. C.; de Souza, T. P.; Lima, E. S.; *Appl. Biochem. Biotechnol.* **2014**, *172*, 311. [Crossref]
37. Wu, C.-H.; Yen, G.-C.; *J. Agric. Food Chem.* **2005**, *53*, 3167. [Crossref]
38. Chinchansure, A. A.; Korwar, A. M.; Kulkarni, M. J.; Joshi, S. P.; *RSC Adv.* **2015**, *5*, 31113. [Crossref]
39. Krutmann, J.; Boulloc, A.; Sore, G.; Bernard, B. A.; Passeron, T.; *J. Dermatol. Sci.* **2017**, *85*, 152. [Crossref]
40. Silva, A. R. A.; de Morais, S. M.; Mendes Marques, M. M.; de Oliveira, D. F.; Barros, C. C.; de Almeida, R. R.; Vieira, Í. G. P.; Guedes, M. I. F.; *Pharm. Biol.* **2012**, *50*, 740. [Crossref]
41. Irda, F.; Nadiya Sahar, A.; Komar Ruslan, W.; *Int. J. Res. Pharm. Sci.* **2014**, *5*, 104. [Link] accessed in November 2024
42. Fidrianny, I.; Rizkiya, A.; Ruslan, K.; *J. Chem. Pharm. Res.* **2015**, *7*, 666. [Link] accessed in November 2024
43. Matsuda, H.; Wang, T.; Managi, H.; Yoshikawa, M.; *Bioorg. Med. Chem.* **2003**, *11*, 5317. [Crossref]
44. Guaratini, T.; Medeiros, M. H. G.; Colepicolo, P.; *Quim. Nova* **2007**, *30*, 206. [Crossref]

Submitted: July 31, 2024

Published online: December 6, 2024